Protistology 14 (4), 191–203 (2020)

Protistology

Morphology and molecular phylogeny of *Aphelidium insulamus* sp. nov. (Aphelida, Opisthosporidia)

Sergey A. Karpov[1,2], Andrey E. Vishnyakov[2], Purificación López-García[3], Natalia A. Zorina[2], Maria Ciobanu[3], Victoria S. Tcvetkova[2] and David Moreira[3]

[1] *Zoological Institute, Russian Academy of Sciences, St. Petersburg 199034, Russian Federation*
[2] *St. Petersburg State University, St. Petersburg 199034, Russian Federation*
[3] *Ecologie Systématique Evolution, CNRS, Université Paris-Saclay, AgroParisTech 91400 Orsay, France*

| Submitted October 5, 2020 | Accepted October 30, 2020 |

Summary

Aphelids remain poorly known parasitoids of algae and have recently raised considerable interest due to their phylogenetic position at the base of Fungi. Accordingly, aphelids may still display some ancestral characters that were subsequently lost in the fungal lineage. Some mycologists consider the aphelids as Fungi. However, unlike Fungi, they are phagotrophs. Molecular environmental studies have revealed a huge diversity of aphelids, but only four genera have been described: *Aphelidium, Amoeboaphelidium, Paraphelidium* and *Pseudaphelidium*. Studying new freshwater aphelid strains by molecular, light and electron microscopy methods, we identified a new aphelid species, *Aphelidium insulamus*. Molecular phylogenetic analysis of the 18S rRNA gene indicates that it is sister to *Aph. melosirae* and, together with *Aph. tribonematis*, they form a monophyletic cluster, which is distantly related to both *Paraphelidium*, with flagellated zoospores, and *Amoeboaphelidium*, with amoeboid zoospores. Ultrastructure of all main life-cycle stages revealed new data for Aphelida cell biology: zoospores and their kinetid (flagellar apparatus) structure, plasmodium, and resting spore. We present the molecular phylogeny of these aphelids using Chytridiomycota as an outgroup.

Key words: Aphelids, Fungi, Holomycota, systematics, taxonomy, ultrastructure

Introduction

Aphelids are intracellular parasitoids of algae that superficially resemble chytridomycetes. However, unlike fungi, they have phagotrophic amoeboid stages in their life cycle (Gromov, 2000; Karpov et al., 2013, 2014a; Letcher et al., 2013). Aphelids were classified in the superphylum Opisthosporidia, which is sister to Fungi and includes members of *Rozella* (Rozellida, Cryptomycota, or Rozellosporidia) and the phylum Microsporidia (Karpov et al., 2014a; Bass et al., 2018). However, a recent phylogenomic study of *Paraphelidium tribonematis* from transcriptome data revealed that the aphelids are sister to Fungi

doi:10.21685/1680-0826-2020-14-4-3

(i.e., Opisthosporidia would not be monophyletic) and, therefore, share a common ancestor with Fungi (Torruella et al., 2018). Although many mycologists include aphelids within Fungi based on molecular analyses (e.g., James et al., 2013; Berbee et al., 2017), evolutionary protistologists exclude aphelids from Fungi (Torruella et al., 2018) because aphelids are phagotrophs, whereas Fungi are osmotrophs. The unique position of aphelids as sister to the Fungi make them a pivotal group of protists and their taxonomy needs to be clarified.

Although only a few aphelid species have been officially described, the group is highly diverse, including many environmental sequences from different ecosystems (Karpov et al., 2013, 2014a), but the number of cultivated species is still low. Currently, only four genera (*Aphelidium, Paraphelidium, Amoeboaphelidium* and *Pseudaphelidium*) have been described with about 20 species in total (Letcher and Powell, 2019).

Because of the phylogenetic and cell biology interest in aphelids, an increasing number of studies about members of this group have been published in recent years. At present, several species have been studied by molecular methods: *Amoeboaphelidium protococcarum* (Karpov et al., 2013; Letcher et al., 2015) and *Am. occidentale* (Letcher et al., 2013, 2015), *Paraphelidium tribonematis* (Karpov et al., 2017a, 2019), and *P. letcheri* (Karpov et al., 2017b), *Aphelidium melosirae* (Karpov et al., 2014 b), *Aph. tribonematis* (Karpov et al., 2016), *Aph. desmodesmi* (Letcher et al., 2017), *Aph. ardennuense* (Tcvetkova et al., 2019), and *Aph. collabens* (Seto et al., 2020). The latter species is in the most basal lineage among cultivated aphelids based on the 18S rDNA phylogenetic tree with Rozellosporidia as sister group. A taxonomic survey of *Aphelidium*, with eight species, and the family Aphelidiaceae has been recently presented (Letcher and Powell, 2019). Although several new species of *Aphelidium* have been recently described, ultrastructure is known for only five of them: *Aph. melosirae* (Karpov et al., 2014b, 2019), *Aph. tribonematis,* and *Aph. chlorococcalium* (Gromov and Mamkaeva, 1975; Karpov et al., 2019), *Aph. desmodesmi* (Letcher et al., 2017), and *Aph. collabens* (Seto et al., 2020). The structure of zoospores and their flagellar apparatus (kinetid) are the most commonly studied traits considered as valid taxonomic characters to map onto the phylogenetic tree. Other stages of the aphelid life cycle, such as the cyst, plasmodium and resting spore have been neglected or considered too difficult for TEM, although they are important for understanding aphelid cell biology and the diversity of eukaryotic cell structure.

Here, we describe the general morphology and ultrastructure of the main life cycle stages of freshwater strains X-133 and X-134 CCPP ZIN RAS with special attention to zoospores, cyst, plasmodium and resting spores. These strains represent the new species *Aphelidium insulamus* sp. nov. as shown by an 18S rDNA-based molecular phylogeny.

Material and methods

Isolation and cultivation of *Aphelidium insulamus* sp. nov.

Strain X-133 and X-134 were isolated by V.S. Tcvetkova from sample 0-11 and 0-14 correspondingly collected from a spring (0-11) and from a ditch (0-14) in the town Ostrov, Pskov Province, Russia in November 2017. We isolated the aphelid strains in two steps: 1) we added a fraction of the water sample to a culture of *Tribonema gayanum* (strain 20 CALU) and checked for infection under the microscope, 2) when algae were infected, we took a zoospore from the culture using a micromanipulator (TransferMan NK2, Eppendorf) and inoculated it into the clean culture with *Tribonema*. Both strains were maintained in culture on *Tribonema gayanum* as described in Karpov et al. (2017a). Light microscopic observations of living cultures were carried out on a Leica Axioplan microscope (Leica Microsystems, St. Petersburg, Russia) equipped with color Axiocam camera (Leica Microsystems, St. Petersburg, Russia).

For transmission electron microscopy (TEM) we used the Method 2 described for *Aph. tribonematis* published in Karpov et al. (2019).

18S rRNA gene amplification, sequencing and molecular phylogenetic analysis

We collected zoospores from the X-133 culture with a micromanipulator and stored each of them in 1 µl of mineral media in PCR-tubes at -21 °C. We added PCR mix (Encyclo Plus PCR kit, Evrogen) directly to the tube. The 18S rRNA gene was amplified with the fungi-like specific primers UF1 (5'-CGAATCGCATGGCCTTG) and AU4 (5'-RTCTCACTAAGCCATTC) (Kappe et al. 1996). PCR amplification program consisted of 5 min denaturation at 94 °C;35 cycles of a denaturation

step at 94 °C for 15 s, a 30 s annealing step at 50 °C and an extension step at 72 °C for 2 min; and a final elongation step of 7 min at 72 °C. After inoculation with the parasite, culture X-134 was incubated for 1–2 weeks to reach the maximum infection of host cells. Zoospores were then collected by a subsequent filtration on a 5 µm then on a 0.45 µm pore-diameter filter. The DNA was extracted from the 0,45 µm filter containing the zoospores, with the Power Soil Kit (Qiagen) following the manufacturer protocol. The 18S rRNA gene was amplified by direct PCR using specific Fungi primers Fun_NS1-F (5'- GTAGTCATATGCTTGTCTC, Vainio and Hantula, 2000) and primer Fun_AU4-R (5'- RTCTCACTAAGCCATTC, Vandenkoornhuyse et al., 2002). 1 µl of DNA was amplified by PCR with the high fidelity polymerase Takara EX Taq (Takara) in a final volume of 25 µl following the manufacturer protocol. Each PCR reaction consisted of 1X polymerase buffer, 0.4mM each dNTP (Eurofins Genomics), 0.4 µM each primer and 0.6U of Takara polymerase. The PCR products were amplified by a Touchdown PCR as follows: 2 min at 94 °C for one cycle, followed by 10 cycles of 30s at 94 °C, 30s at 65 °C, 75s at 72 °C while decreasing annealing temperature by 1 °C each cycle. Next, 25 cycles of 30s at 94 °C, 30s at 55 °C and 75s at 72 °C, followed a final extension 5 min at 72 °C. Negative controls without template DNA were used at all amplification steps. Fragments of the expected size were used for Sanger sequencing.

The new 18S rRNA gene sequences were aligned with a collection of sequences of available aphelids and several Chytridiomycota species as outgroup using Mafft (Katoh et al., 2002) with default parameters. The multiple alignment was then manually trimmed to eliminate gaps and ambiguously aligned sites. 1,414 unambiguously aligned sites were retained to reconstruct a phylogenetic tree by Maximum Likelihood (ML) using IQ-TREE 2 (Minh et al., 2020) with the GTR+G+I sequence evolution model. The new 18S rRNA gene sequences have been deposited in GenBank with accession numbers MW354078 (strain X-133), MW186929 (strain X-134).

Results

Molecular phylogeny

We amplified and sequenced a near-full 18S rRNA gene from the strains X-133 and X-134 of *Aph. insulamus* sp. nov. (CCPP ZIN RAS) maintained in culture on the xanthophyte alga *Tribonema gayanum* (strain 20 CALU). Both sequences were nearly identical to each other and certainly belong to the same species *Aph. insulamus* sp. nov. Sequences of the new species were 90% identical to those of another described *Aphelidium* species, *Aph. melosirae*, suggesting that they are two closely related *Aphelidium* species. We reconstructed a maximum likelihood (ML) phylogenetic tree including the new 18S rDNA sequences and a selection of aphelid sequences together with several Chytridiomycota sequences as outgroup (Fig. 1). In our tree, *Aph. insulamus* sp. nov. formed a clade with *Aph. melosirae* with strong statistical support (bootstrap value of 86% according to ML phylogeny). This clade is sister to the aphelid species *Aph. tribonematis* and *Aph. arduennense* forming a monophyletic branch that includes the most basal *Aph. collabens* and some environmental sequences. Outside of this clade is *Aph. desmodesmi*, which clusters with *Amoeboaphelidium* making *Aphelidium* paraphyletic (see Discussion).

Life cycle (light microscopy)

The life cycle of *Aph. insulamus* sp. nov. corresponds to that described for other *Aphelidium* species. The zoospores have a slightly elongated body 2.0-4.0 (average3,06) µm long, 1.6-2.2 (average 1.91) µm width, and a flagellum 7.4-10.6 (average 8.84) µm including an acroneme of 1.2-1.8 (average 1.38) µm (Fig. 2, A-D). Seven zoospores were measured. Swimming zoospores have oval or round outlines, but when stopped near a substrate they produce filopodia or anterior lamellipodium and move like amoebae. They can totally retract the flagellum and use filopodia for movement (Fig. 2, E, F). Both flagellated and amoeboid zoospores can attach to the host alga, and encyst (Fig. 2, G, H). The cyst germinates and penetrates the host cell wall with an infection, or penetration tube. The so-called posterior vacuole appears in the cyst and grows pushing out the cyst contents through the penetration tube into the host (Fig. 2, G). Some peripheral cytoplasm remains in the nearly empty cyst (Fig. 2, H), while the main part of the parasitoid cell is in the host and becomes a trophont, which engulfs the host cytoplasm forming a central vacuole (Fig. 2, I). The parasitoid grows and forms a plasmodium that totally replaces the host cytoplasm (Fig. 2, J, K). This multinucleate plasmodium has a large central vacuole containing a residual excretion

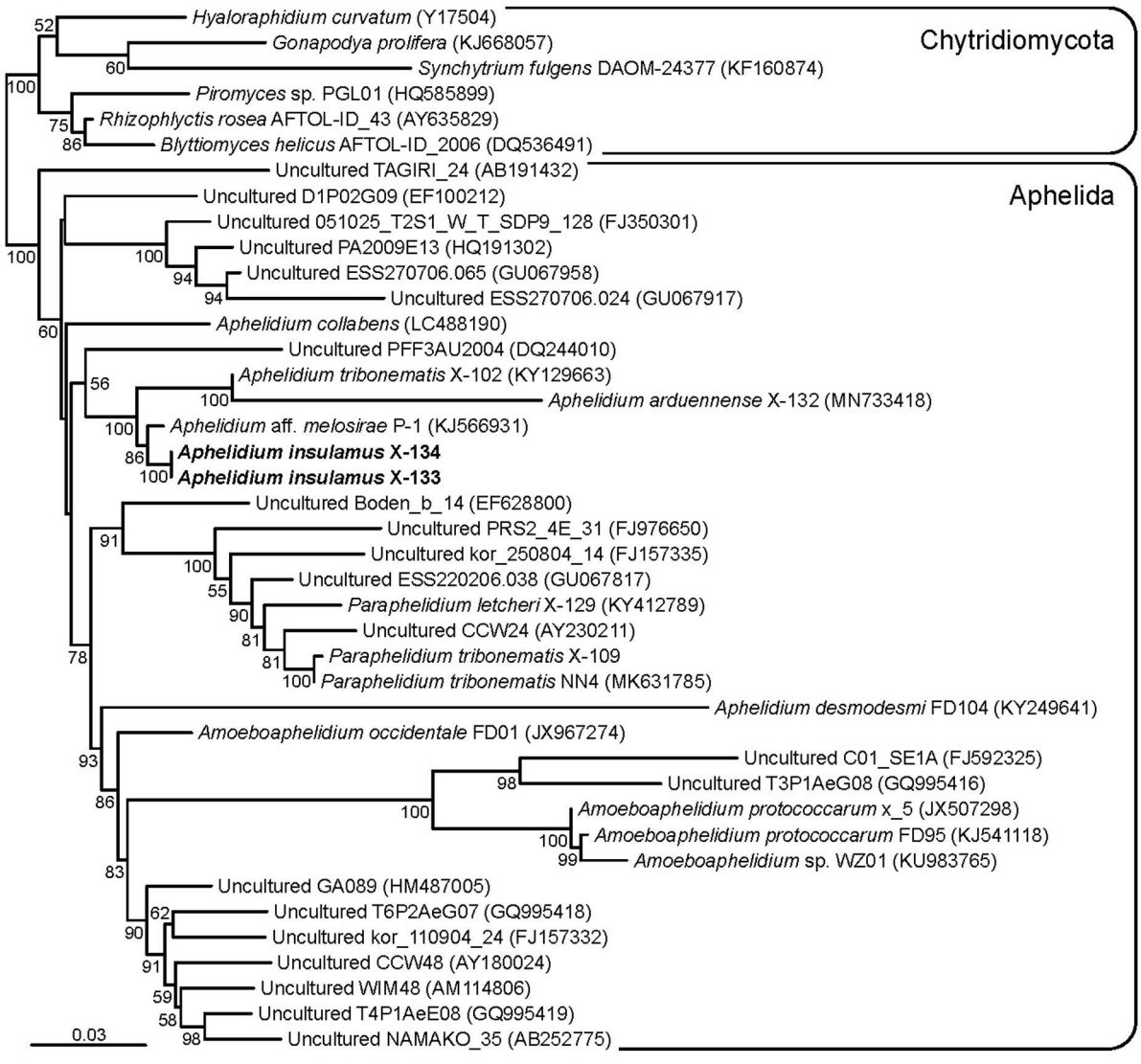

Fig. 1. 18S rDNA-based Maximum Likelihood phylogenetic tree showing the position of *Aphelidium insulamus*. The aphelid tree was rooted using chytrid fungal sequences. The tree was constructed using 1414 conserved positions. Numbers at branches are bootstrap values.

body represented by one big or several lipid globules of varying diameter. The mature plasmodium divides into a number of uninucleate cells (Fig. 2, L), which become zoospores. Zoospores develop flagella inside the sporangium and release from the empty host cell probably one by one through the gap between the halves of the algal wall, or several cells can come out simultaneously when the host wall is broken. A few zoospores often stay in the host envelope for some time.

The mature resting spore is spherical, has one or two large lipid globules, and is covered with a smooth thick wall. A residual body is normally attached to the outer surface of the resting spore wall located inside the outer thin envelope (Fig. 2, O-Q). We observed several stages of resting spore maturation in culture (Fig. 2, M-Q). At first the plasmodium ejects the residual body and the central vacuole migrates to the end of the cell (Fig.2, M), the cytoplasm becomes dense and granulated with a lateral lipid globule, and the cell produces a noticeable covering (Fig. 2, N, O). At the next stage the vacuole disappears, the granular cytoplasm becomes homogenous, and one or two lipid globules localize at the ends of the slightly elongated compact cell, which is covered with a thick and dense wall (Fig. 2, O-Q). An outer envelope around the mature resting spore and residual body is rather conspicuous (Fig. 2, O).

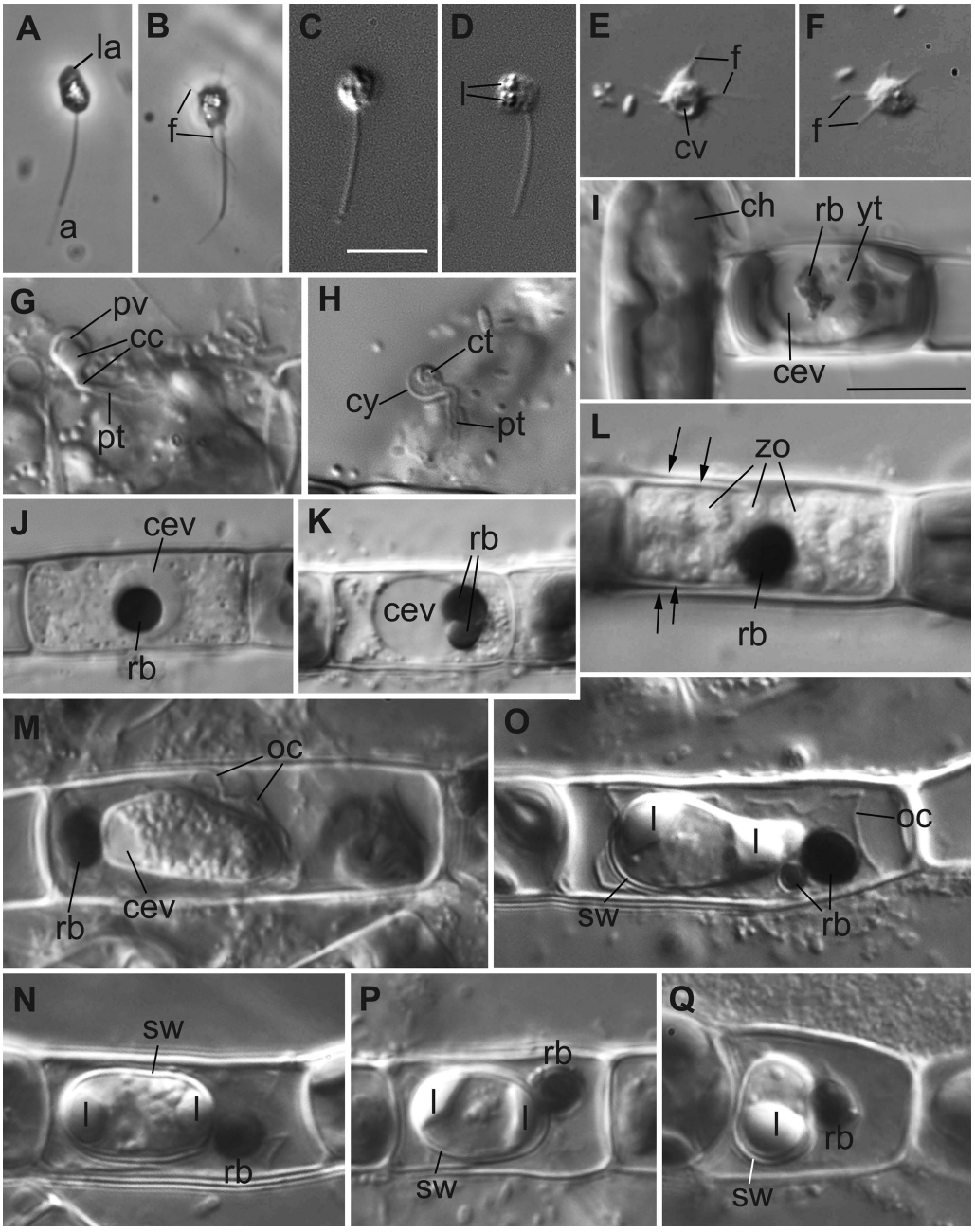

Fig. 2. Main stages of the life cycle of *Aphelidium insulamus* (A,B,E,F,G-L,O: X-133, others: X-134) observed in living material by phase (A, B) and differential interference contrast (DIC) microscopy. A-D – Flagellated, E-F – aflagellated zoospores with filopodia; G – cyst on the *Tribonema* filament with penetration tube during migration of its contents into the host; H – empty cyst and penetration tube with remnants of cytoplasm in the cyst; I – healthy cells of the host (to the left), young trophont of parasitoid with central vacuole; J-K – plasmodium stage with central vacuole containing residual body; L – mature sporangium with cleaved zoospores and residual body; *arrows* show the halves of host cell wall; M-Q –stages of resting spore maturation from elongated cell with terminal vacuole (M), further reduction of size and shape changing (N), surrounded by outer covering and spore wall (O); the residual body lies in between the outer covering and spore wall. *Abbreviations*: a – acronema, cc – cyst contents, cev – central vacuole, ch – chloroplast, ct – remnants of cytoplasm, cv – contractile vacuole, cy – cyst, f – filopodium, l – lipid globule, la – lamellipodium, oc – outer covering, pt – penetration tube, pv – posterior vacuole, rb – residual body, sw – spore wall, yt – young trophont, zo-zoospores. Scale bars: in C for A-F = 5 μm; in I for I-Q = 10 μm.

Ultrastructure of zoospores

Both mature zoospores inside the sporangium (Fig. 3, B) and released zoospores (Fig. 3, A, C) have the same morphology. The elongated curved nucleus of *Aph. insulamus* sp. nov. locates in the middle/posterior part of the cell is normally shifted to one side. A contractile vacuole is located in the posterior half of the cell (Figs 3, B, C; 5, B, C; S1). A vacuole with some excreted material is present adjacent the nucleus (Fig. 3, B, C). The cytoplasm contains multiple mitochondria with lamellar cristae and numerous ribosomes dispersed throughout the cytoplasm (Fig. 3, A-G). Small lipid globules are situated around the nucleus. A rather prominent sac-like microbody with granular contents lies anteriorly between two-three lipid globules, forming a microbody-lipid complex (MLC) that is often associated with mitochondrial profiles (Figs 3, D; S1). A Golgi apparatus lies anterior to the flagellar base (Figs 3, A; 5, A-C; S1). Figure 3 E-G illustrates the amoeboid nature of zoospores; filopodia are supported by bundles of microfilaments and can be extremely flexible, enabling zoospores to crawl on the algal surface (Fig. 3, G).

Zoospores can easily retract a flagellum. The retracted axoneme coils around the cell contents in the peripheral cytoplasm (Fig. 3, E, G). The ultrastructural evidence for flagellar retraction process corresponds to our previous light microscopic observations for *Aph. tribonematis* (Karpov et al. 2016): the cell stops, revolves and reels up the flagellum from the base to the tip submerging the axoneme in the cell. This process places the axoneme in the peripheral cytoplasm, as seen in Fig. 3, E, G. In some amoeboid zoospores the nucleus is elongated into a long pseudopodium suggestive a cyst with long penetration tube, yet without a cyst envelope (Fig. 3, G).

Cyst

The cyst is the next stage in the aphelid life cycle. The rounded aflagellated cell produces a relatively thin wall and germinates with penetration tube into the host (Fig. 3, H, K). The tube grows in between the halves of *Tribonema* cell wall to reach the host plasma membrane (Fig. 3, K). The vacuole appears in the cyst and enlarges (Fig. 3, H-K). At the first stage the vacuole is small and filled with numerous small vesicles, then it enlarges and migrates to the cell periphery (Fig. 3, H, I). The progressive vacuole enlargement, which is accompanied by the disappearance of small vesicles in the vacuole, pushes the cyst contents through the tube out of the cyst (Fig. 3, K). A thin layer of cytoplasm remains in the cyst covering the inside of the cyst wall. Interestingly, unreleased zoospores may encyst on the inner surface of the host cell wall and try to penetrate it from inside (Fig. 3, J), having no chance to proliferate.

Trophont

Once inside the host the cyst contents become amoeboid and engulf host cytoplasm including organelles. At the very early stage, it forms a central vacuole for digestion and accumulation of the residual body (Fig. 3, L). The trophont grows and becomes a plasmodium with numerous nuclei and a huge central vacuole containing at least one big lipid granule often ornamented with a reticulate substance (Fig. 4, B, D). The plasmodium totally replaces the host cell and lies on amorphous matrix restricted by an outer membrane that belongs to the host (Fig. 4, A-D).

Mature sporangium

The plasmodium divides into separate cells and the future zoospores each produce a flagellum (Fig. 4, E). When zoospore formation is complete, an outer membrane disappears (Fig. 4, E), probably, zoospore movement breaks it. Zoospores can move inside the host cell wall and then release through the gap between the host wall halves.

Resting spore

The resting spore of *Aphelidium insulatus* sp. nov. and the residual body normally appear inside the outer membrane (Fig. 4, F, G). The resting spore has a thick wall with an electron dense outer layer, its plasma membrane has folded appearance delimiting a rather dense cytoplasm (Fig. 4, F-H). On some sections the huge lipid globule, nucleus, numerous mitochondria and small lipid globules can be observed (Fig. 4, H).

Kinetid structure

The kinetid, or flagellar apparatus, contains a kinetosome attached to the flagellum and a non flagellar kinetosome, or centriole (Figs 5; S1). The

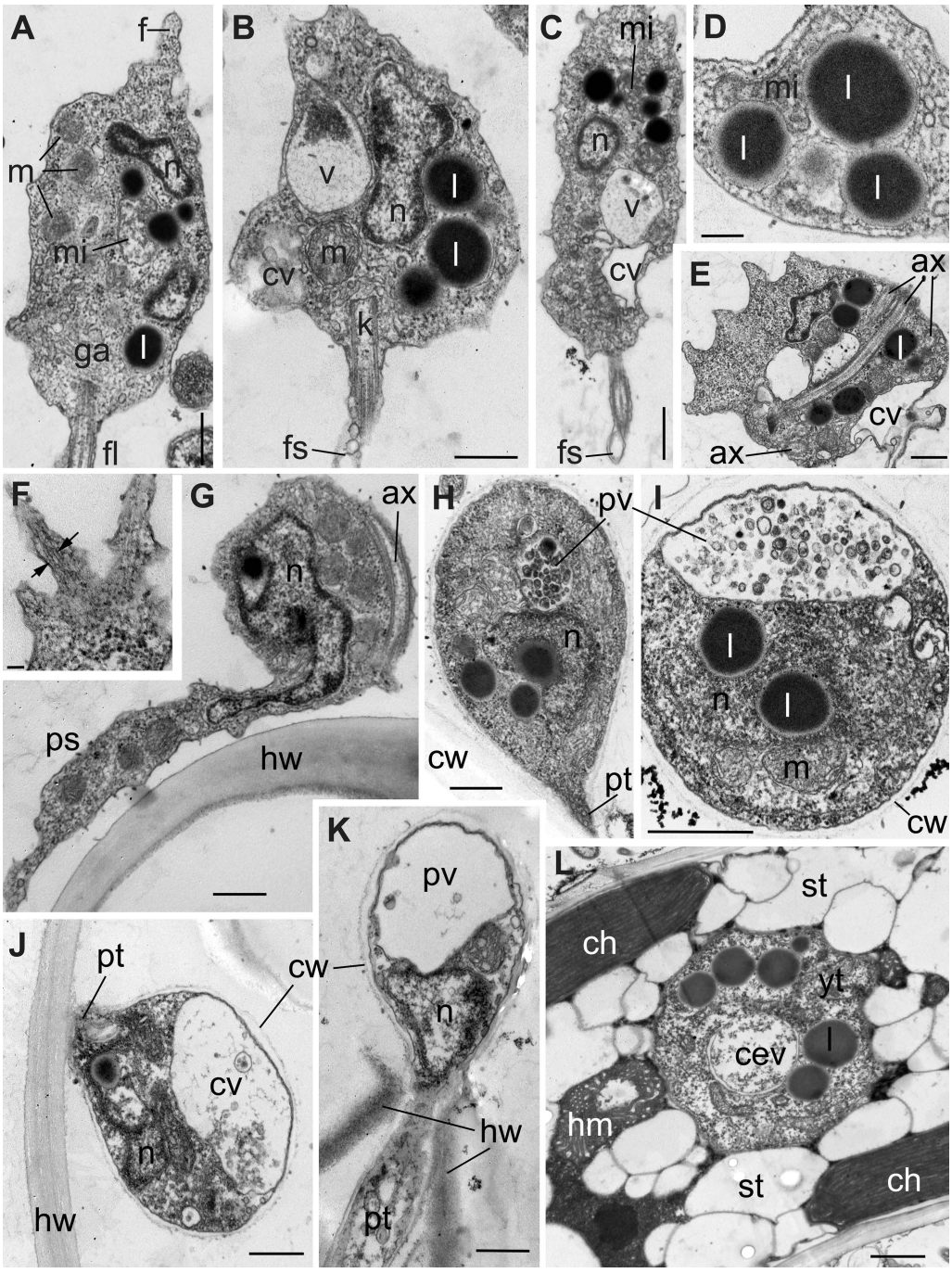

Fig. 3. Ultrastructure of released zoospores (A-G), cysts (H-K) and young trophont (L) of *Aphelidium insulamus* (C,G: X-133, others: X-134). A-D – Organelle disposition in the flagellated zoospores: released (A, C) and intrasporangial (B); D – microbody-lipid complex; E – amoeboid zoospore with recently retracted flagellum; F – microfilaments in filopodia; G – flexibility of nucleus in amoeboid zoospore with retracted flagellum; H, I – cysts with growing multivesiculated vacuole; J – encysted zoospore inside empty host cell; K – cyst with penetration tube in between the halves of *Tribonema* cell wall; L – young trophont in the host cell. *Abbreviations*: ax – axonema, cw – cyst wall, ga – Golgi apparatus, hm – host mitochondrion, hw – host cell wall, m – mitochondrion, mi – microbody, n – nucleus, ps – pseudopodium, st –starch granule, v – vacuole; other abbreviations as in Fig. 2. Scale bars: A-E – 500 nm, F – 200 nm, G-K – 500 nm, L – 1 μm.

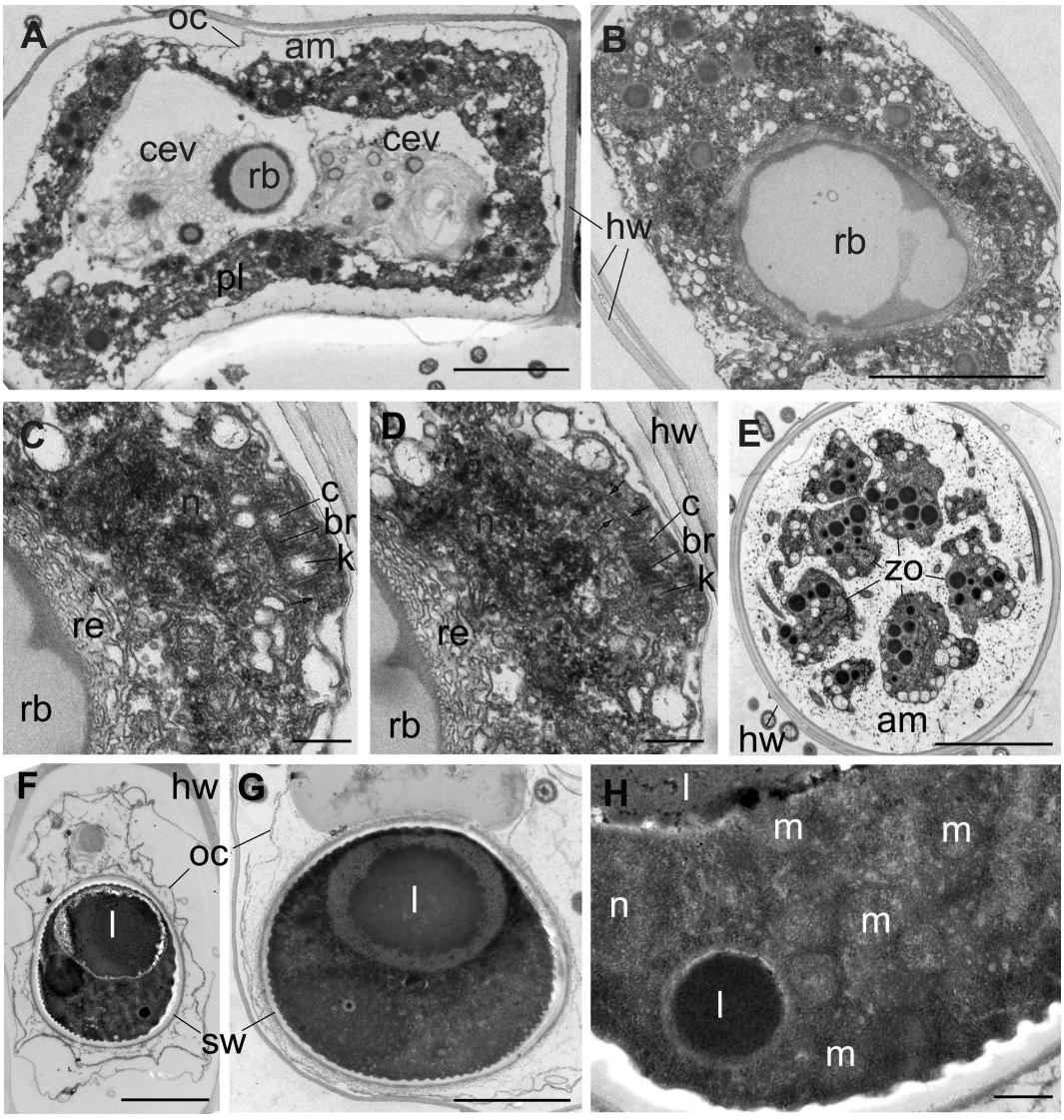

Fig. 4. Ultrastructure of the plasmodium (A-D), mature sporangium (E) and resting spore (F-H) of *Aphelidium insulamus* (X-134). A – Plasmodium with huge central vacuole; B – multinucleate plasmodium with compact central vacuole filled with residual body; C, D – two consecutive sections show parallel orientation of centrioles with radiating microtubules; E – mature sporangium with flagellated zoospores; F, G – two resting spores with outer covering and spore wall; H – portion of resting spore with nucleus, mitochondria and lipid globules. *Abbreviations*: am – amorphous matrix, br – bridge between kinetosome and centriole, c – centriole, k – kinetosome, oc – outer covering, pl – plasmodium, re – reticulate envelope covering a residual body; other abbreviations as in Figs 2 and 3. Scale bars: A,B,E,F – 3 μm, C,D,H – 300 nm, G – 2 μm.

free part of the flagellum has a typical 9+2 axoneme. The flagellum has an acroneme at the distal end and an unusual swelling filled with vesicles at its base (Figs 3, B, C; 5, A, B). The swelling locates at one side of flagellum and often has a posterior projection (Fig. 5, B). The transition zone of the flagellum contains a very thin transverse plate 150 nm above the cell surface (Fig. 5, B) where the central tubules of the axoneme also start. A spiral filament is present in the transition zone between transverse plate and cell surface (Fig. 5, G, H). The kinetosome is 200-250 nm long, is composed of microtubular triplets, and contains a cartwheel structure (Fig. 5, B). The centriole is extremely short (50-60 nm) and composed of triplets of peripheral microtubules with cartwheel structure (Fig. 5, J). It lies at an angle of 45°-60° with respect to the kinetosome (Figs 5, C, J, K; S1,D-G). A broad fibrillar bridge connects

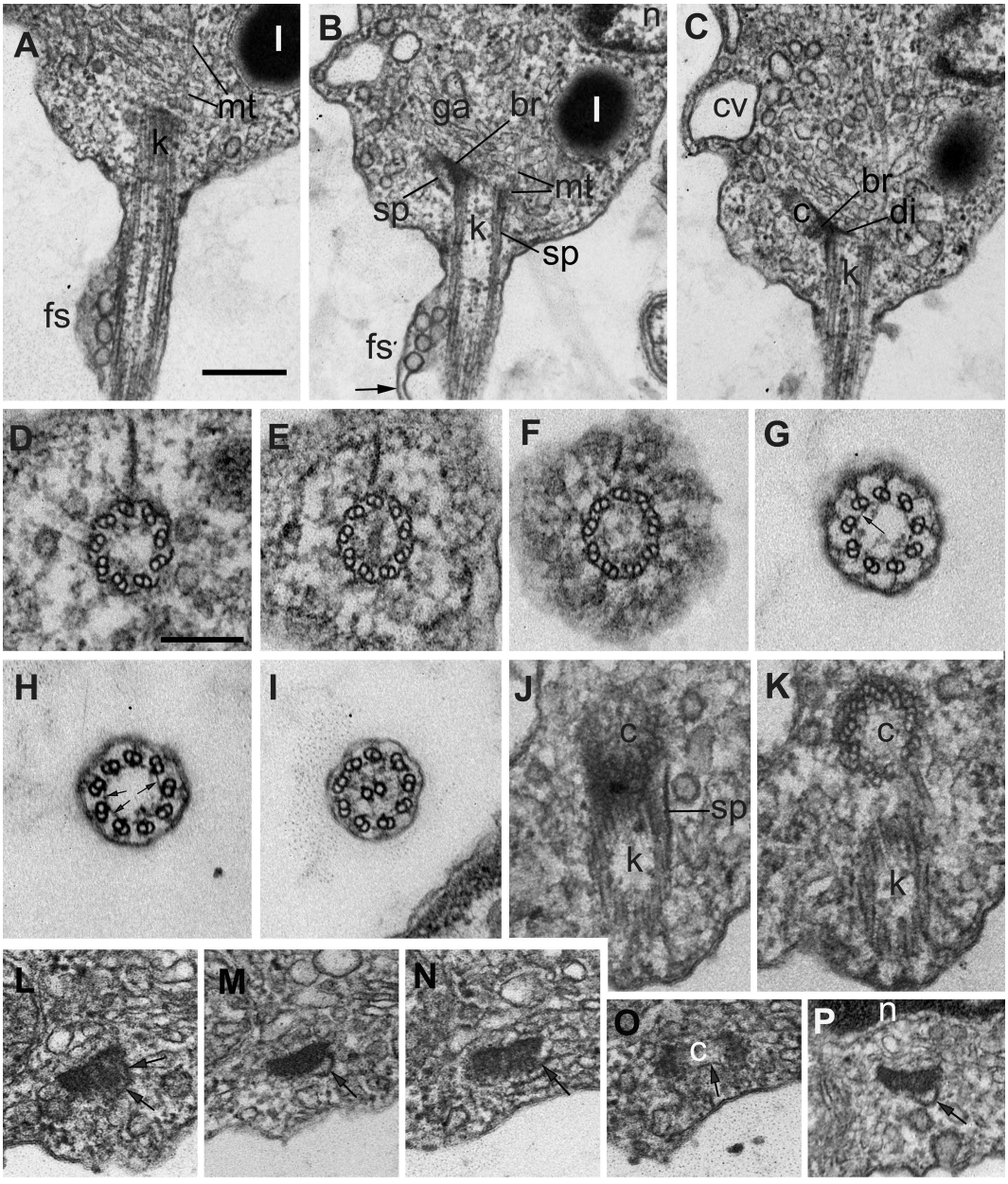

Fig. 5. Kinetid structure of *Aphelidium insulamus* (D-K,P: X-133, others: X-134). A-C – Series of consecutive longitudinal sections of posterior end of the cell through flagellar apparatus, *arrow* in B shows a posterior projection of flagellar swelling; D-I – series of consecutive transverse sections of flagellar transition zone, *arrows* on G, H show a spiral filament; J, K – two consecutive transversal sections of centriole; L-O – series of consecutive transversal sections of the kinetosome-centriole bridge with spur, and LS of centriole (O); P – section of the bridge of strain X-133 at the same place as in M (strain X-134) confirms kinetid identity of two strains, *arrows* show a spur. *Abbreviations*: di – diaphragm, fs – flagellar swelling, mt – microtubules, sp – spur; other abbreviations as in Figs 2-4. Scale bars: A-C – 400 nm, D-M – 200 nm.

the lateral parts of the kinetosome and the centriole (Figs 5, C, J, L-P; S1, D-G). A thin plate passes from kinetosome to centriole along the bridge (Figs 5, B, J, L-N, P; S1, F). It has rather peculiar shape that can be interpreted as a spur.

Microtubular roots were not found in kinetid of *Aph. insulamus* sp. nov.; however, several single microtubules, predominantly oriented anteriorly into the cytoplasm, originate from the kinetosome surface opposite the bridge (Fig. 5, J–M).

Schematics of zoospore organization and kinetid structure of *Aph. insulamus* sp. nov. are shown in Fig. 6.

Taxonomy

Aphelidium insulamus Karpov, Zorina et Moreira sp. nov. (Fig. 2).

Index Fungorum number: IF557966

Etymology. Latin epithet of the Russian town name Ostrov (=Island) where the samples were collected.

Swimming zoospores with spherical or elongated body 2-4 μm long with several small lipid globules and posterior contractile vacuole. Flagellum 7-10 μm in length including an acroneme of 1-1.8 μm, a vesiculated swelling, and a spiral filament in the flagellar transition zone. Flagellated zoospores can produce filopodia, an anterior lamellipodium, and can easily retract the flagellum and move as amoebae. Resting spores spherical or elongated 6-8 μm in diameter with smooth wall; containing one or two big lipid globules.

Type. Fig. 2, C,D, M, N, P, Q this publication. Isolated from samples 0-14 by Victoria Tcvetkova in Russia, Pskov Province, town Ostrov 57°34′35″N; 28°35′15″W. Sample collected in November 2017. Ex type culture deposited in ZIN collection (CCPP ZIN RAS) under No: X-134.

Note. The *Aph. insulamus* differs from its closest relative *Aph. melosirae* by approximately twice smaller zoospore body and flagellum, presence of flagellar swelling, and absence of basal foot of kinetosome initiating microtubules (Table 1).

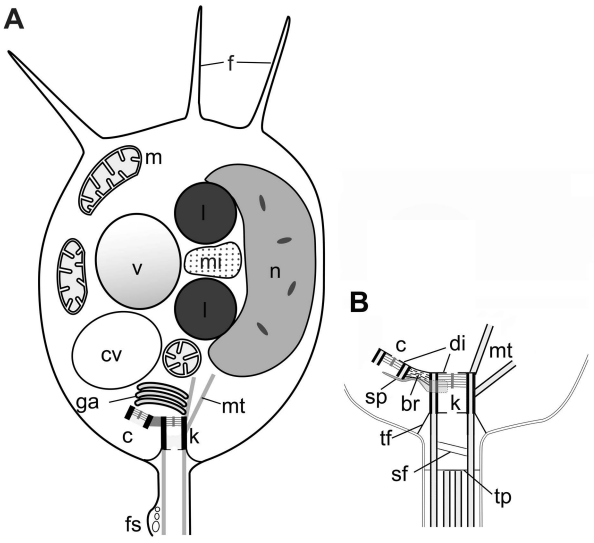

Fig. 6. Scheme of zoospore (A) and kinetid structure (B) of *Aphelidium insulamus. Abbreviations*: sf – spiral filament, tf – transition filament, tp – transverse plate; other abbreviations as in Figs 2-5.

Discussion

Molecular phylogeny

Both strains have nearly identical SSU rDNA, providing convincing evidence that X-133 and X-134 belong to one species. The *Aph. insulamus* 18S rRNA gene sequence differs from that of its neighbor species *Aph. melosirae* by 10%. Nonetheless, both species are closely related to each other forming a clade fitting well in the aphelid species cluster. In spite of the use of a different outgroup than in earlier studies (the closer chytridiomycetes instead of the previously used rozellids) the tree topology retains three main clusters, with cultured species corresponding to the genera *Aphelidium*, *Paraphelidium* and *Amoeboaphelidium* (Karpov et al., 2019; Tcvetkova et al., 2019; Seto et al., 2020). The genetic divergence between 18S rRNA genes of *Aphelidium* morphospecies is also quite high for species level: 16% dissimilarity between *Aph. insulamus* and *A. tribonematis* sequences, and 14% between *Aph. melosirae* and *Aph. tribonematis* (Karpov et al., 2016). This high degree of divergence within a genus might be possibly related to the fact that parasite genes tend to evolve faster than those of free-living species; however, the species level divergence in highly specialized and fast evolved parasites like Microsporidia is about 1-2% (Kyei-Poku and Sokolova, 2017). Thus, the reason might be the understudied diversity of the aphelids.

The two most basal aphelid clusters consist of environmental sequences, and the next one by the recently described *Aph. collabens* (Seto et al., 2020). One more *Aphelidium* species, *Aph. desmodesmi*, is in the *Amoeboaphelidium* cluster. This paraphyly of the genus *Aphelidium* can be seen in all molecular phylogenetic trees published up to now (e.g. Karpov et al., 2019; Seto et al., 2020). In 18S rDNA sequence analyses *Aph. desmodesmi* is always on the longest branch with only low to moderate support. This may suggest that its anomalous position on the tree may be because of LBA effect. More aphelids similar to *Aph. desmodesmi* need to be found and sequenced to solve this problem.

Table 1. Comparison of zoospore characters of *Aphelidium* spp. Data obtained from the original taxonomic descriptions and present paper.

Character/Species	*Aph. desmodesmi* (Letcher et al., 2017)	*Aph. chlorococcalium* (Karpov et al., 2019)	*Aph. melosirae* (Karpov et al., 2019)	*Aph. insulamus* (present paper)	*Aph. tribonematis* (Karpov et al., 2016, 2019)	*Aph. collabens* (Seto et al., 2020)
Zoospore diameter (length) (μm)	1.6–1.9	3–4	4–6	2–4	3–3.5	1.8–2.5
Length of flagellum (μm)	6	10–12	15	7.4–10.6	10–12	6.0–7.5
Mitochondria appressed to nucleus	–	+	–	–	–	–
Kinetosome composition	triplets	triplets	triplets	triplets	triplets	doublets
Centriole location to kinetosome	Orthogonal or sharp angle	Orthogonal	Sharp angle	Sharp angle	Sharp angle	Sharp angle
Length of kinetosome (nm)	200	250–300	300	250–300	200	–
Length of transition zone (nm)	250–300	50–100	?	150	400	?
Swelling at the flagellar base	–	–	–	+	–	–
Coiled fiber in transition zone	+?	–	+	+	–	–
Microtubule producing foot opposite to centriole	+ (Fig. 3F)	+	+	–	+	–?
Microtubular root	–	–	–	–	–	+
Kinetosome connected to mitochondrium with fibrillar root	–	+	?	–	–	–
Fibrillar root	–?	+	?	–	–	+
Spur	–	–	+ (Fig. 2, I)	+	–	–

Ultrastructural comparisons

Comparative ultrastructure of all life-cycle stages during the study of aphelid new species description gives valuable information on the cytology and understanding the biology of these interesting but still understudied parasitoids of algae.

Kinetid structure

The kinetid of *Aph. insulamus* is similar to the recently studied kinetid of *Aph. tribonematis* and *Aph. melosirae* (Karpov et al., 2019). All have the centriole oriented at a sharp angle with respect to the kinetosome, with microtubular singlets at the opposite side, and have no fibrillar root (Table 1). *Aph. insulamus* has no basal foot, but has a spiral filament in the transition zone, like *Aph. melosirae*, which is sister to *Aph. insulamus* in the phylogenetic tree (Fig. 1). Also, the kinetosome of both species has a spur, which is visible in *Aph. melosirae* (Fig. 2l in Karpov et al., 2019), and is absent in other *Aphelidium* species (Gromov and Mamkaeva, 1975; Letcher et al., 2017; Karpov et al., 2019; Seto et al., 2020).

In general, the kinetid structure reflects phylogenetic relationships in the genus *Aphelidium*. The most basal branch, *Aph. collabens*, has the most complex kinetid with a microtubular root, which is absent in other *Aphelidium* spp., including *Aph. chlorococcalium* (with no 18S rRNA gene sequence available, see Karpov et al., 2019) and a prominent rhizoplast (Table 1). *Aph. insulamus* has the simplest set of kinetosomal derivatives; it has lost even a basal foot on the kinetosome surface producing microtubules. Kinetosomes probably differ in *Aph. desmodesmi*, but it is not clear because dense cytoplasm masked the cytoskeletal elements in previous studies (Letcher et al., 2017).

The swelling at the flagellar base occurs in zoospores of both strains of *Aph. insulamus*. The unusual vesiculated nature with a posterior projection

might be a result of amoeboid activity, for example, temporary filopodial growth, but it was present in all studied zoospores and seems to be a permanent structure. This swelling is a unique character within *Aphelidium* (Table 1), and, probably, for zoospores of all aphelids; however, a similar structure occurs on the flagella of intrasporangial zoospores of *Rozella allomycis* (Powell and Letcher, 2019).

The other life cycle stages of *Aph. insulamus* are similar to those of the aphelids in general. Aphelid cell structures have been investigated in most detail for *Aph. melosirae* (Karpov et al., 2014b), therefore we discuss here some aphelid peculiarities using those data.

Cyst

A so-called posterior vacuole grows due to the process of vesicle accumulation inside the vacuole, which disappears later probably using their membranes for a vacuole growth. Migration of cyst contents into the host may be a result of pressure from vacuole growth or microtubular mediated transport of cytoplasmic organelles and nucleus through the penetration tube (the cytoplasm passing through penetration tube contains microtubules; Karpov et al., 2014b).

Resting spore

The thick wall of aphelid resting spores has not allowed adequate penetration of TEM fixatives, therefore its internal structure was not studied. However, we found a few sections with more or less suitable images of *Aph. insulamus* spores. These resting spores contain numerous mitochondria, one, or probably a few nuclei distinguishable within the dense cytoplasm background by their double membrane envelope, and 1-2 big lipid globules plus several small ones. Using the fixative with potassium permanganate and osmium tetroxide for fixation of *Amoeboaphelidium chlorellavorum*, Gromov and Mamkaeva (1970) demonstrated in its resting spore one or two nuclei, mitochondria, and unusual vacuoles with electron translucent contents, probably, starch granules taken from the *Chlorella* host. Lipid granules were absent in the spore.

Resting spore derives straight from the plasmodium, which contains several nuclei. The central vacuole moves to the cell periphery and ejects the residual body into the space between host plasma membrane and plasmodium envelope. The plasmodium produces a thick wall and becomes the resting spore. The number of nuclei in the resting spore is unclear, as is their behavior during transformation from plasmodium to spore.

Acknowledgments

This study was supported by RSF grant No. 16-14-10302. We thank I.R. Pozdnyakov for help with drawing the Fig. 6, the Research Resource Center for Molecular and Cell Technologies (RRC MCT), and the Biobank at St. Petersburg State University (SPbSU) for access to the EM facilities and sequencing.

References

Bass D., Czech L., Williams B.A.P., Berney C., Dunthorn M. et al. 2018. Clarifying the relationships between Microsporidia and Cryptomycota. J. Eukaryot. Microbiol. 65, 773–782.

Berbee M.L., James T.Y. and Strullu-Derrien C. 2017. Early diverging fungi: diversity and impact at the dawn of terrestrial life. Annual Review of Microbiology, 71, 41–60.

Gromov B.V. 2000. Algal parasites of the genera *Aphelidium, Amoeboaphelidium* and *Pseudoaphelidium* from the Cienkovski's "Monadea" group as representatives of new class. Zool. Zhurn. 79, 517–525 (in Russian with English summary).

Gromov B.V. and Mamkaeva K.A. 1970. The cycle of development and mode of nutrition of *Amoeboaphelidium chlorellavorum* - an intracellular parasite of *Chlorella*. Tsitologiya. 12, 1191–1194 (in Russian with English summary).

Gromov B.V. and Mamkaeva K.A. 1975. Zoospore ultrastructure of *Aphelidium chlorococcarum* Fott. Mikol. Fitopatol. 9, 190–193 (in Russian with English summary).

James T.Y., Pelin A., Bonen L., Ahrendt S., Sain D. et al. 2013. Shared signatures of parasitism and phylogenomics unite Cryptomycota and microsporidia. Curr. Biol. 19, 1548–1553.

Karpov S.A., Mikhailov K.V., Mirzaeva G.S., Mirabdullaev I.M., Mamkaeva K.A. et al. 2013. Obligately phagotrophic aphelids turned out to branch with the earliest-diverging fungi. Protist. 164, 195–205.

Karpov S.A., Mamkaeva M.A., Aleoshin V.V., Nassonova E., Lilje O. and Gleason F.H. 2014a. Morphology, phylogeny, and ecology of the aphelids (Aphelidea, Opisthokonta) and proposal for the new

superphylum Opisthosporidia. Front. Microbiol. 5, 112.

Karpov S.A., Mamkaeva M.A., Benzerara K., Moreira D. and López-García P. 2014b. Molecular phylogeny and ultrastructure of *Aphelidium* aff. *melosirae* (Aphelida, Opisthosporidia). Protist. 165, 512–526.

Karpov S.A., Mamkaeva M.A., Moreira D. and López-García P. 2016. Molecular phylogeny of *Aphelidium tribonemae* reveals its sister relationship with *A.* aff. *melosirae* (Aphelida, Opisthosporidia). Protistology. 10, 97–103.

Karpov S.A., Tcvetkova V.S., Mamkaeva M.A., Torruella G., Timpano H. et al. 2017a. Morphological and genetic diversity of Opisthosporidia: new aphelid *Paraphelidium tribonemae* gen. et sp. nov. J. Eukaryot. Microbiol. 64, 204–212.

Karpov S.A., Torruella G., Moreira D., Mamkaeva M.A. and López-García P. 2017b. Molecular Phylogeny of *Paraphelidium letcheri* sp. nov. (Aphelida, Opisthosporidia). J. Eukaryot. Microbiol. 64, 573–578.

Karpov S.A., Cvetkova V.S., Annenkova N.V. and Vishnyakov A.E. 2019. Kinetid structure of *Aphelidium* and *Paraphelidium* (Aphelida) suggests the features of the common ancestor of Fungi and Opisthosporidia. J. Eukaryot. Microbiol. 66, 911–924.

Kappe R., Fauser C., Okeke C.N. and Maiwald M. 1996. Universal fungus-specific primer systems and group-specific hybridization oligonucleotides for 18S rDNA. Mycoses. 39, 25–30.

Katoh K., Misawa K., Kuma K. and Miyata T. 2002. MAFFT: a novel method for rapid multiple sequence alignment based on fast Fourier transform. Nucleic Acids Res. 30, 3059–3066.

Kyei-Poku G. and Sokolova Y.Y. 2017. The microsporidium *Nosema disstriae* (Thomson 1959): fine structure and phylogenetic position within the *N. bombycis* clade. J. Invertebr. Pathol. 143, 90–103.

Letcher P.M., Lopez S., Schmieder R., Lee P.A., Behnke C. et al. 2013. Characterization of *Amoeboaphelidium protococcarum*, an algal parasite new to the Cryptomycota isolated from an outdoor algal pond used for the production of biofuel. PLoS ONE 8, e56232.

Letcher P.M., Powell M.J., Lopez S., Lee P.A. and McBride R.C. 2015. A new isolate of *Amoeboaphelidium protococcarum*, and *Amoeboaphelidium occidentale*, a new species in phylum Aphelida (Opisthosporidia). Mycologia 107, 522–531. doi:10.3852/14-064.

Letcher P.M. and Powell M.J. 2019. A taxonomic summary of Aphelidiaceae. IMA Fungus 1, 4.

Letcher P.M., Powell M.J., Lee P.A., Lopez S. and Burnett M. 2017. Molecular phylogeny and ultrastructure of *Aphelidium desmodesmi*, a new species in Aphelida (Opisthosporidia). J. Eukaryot. Microbiol. 64, 655–381.

Minh B.Q., Schmidt H.A., Chernomor O., Schrempf D., Woodhams M.D. et al. 2020. IQ-TREE 2: New models and efficient methods for phylogenetic inference in the genomic era. Mol. Biol. Evol. 37, 1530–1534.

Powell M.J. and Letcher P.M. 2019. Ultrastructure of early stages of *Rozella allomycis* (Cryptomycota) infection of its host, *Allomyces macrogynus* (Blastocladiomycota). Fungal Biology, 123, 109–116.

Seto K., Matsuzawa T., Kuno H. and Kagami M. 2020. Morphology, ultrastructure, and molecular phylogeny of *Aphelidium collabens* sp. nov. (Aphelidiomycota), a parasitoid of a green alga *Coccomyxa* sp. Protist. 171, 125728. https://doi.org/10.1016/j.protis.2020.125728.

Tcvetkova V.S., Zorina N.A., Mamkaeva M.A. and Karpov S.A. 2019. Molecular phylogeny of *Aphelidium arduennense* sp. nov. - new representative of Aphelida (Opisthosporidia). Protistology. 13, 192–198.

Torruella G., Grau-Bové X., Moreira D., Karpov S.A., Burns J.A. et al. 2018. Global transcriptome analysis of the aphelid *Paraphelidium tribonemae* supports the phagotrophic origin of fungi. Commun. Biol. 1, 231.

Vainio E. and Hantula J. 2000. Direct analysis of wood-inhabiting fungi using denaturing gradient gel electrophoresis of amplified ribosomal DNA. Mycol. Res. 104, 927–936.

Vandenkoornhuyse P., Baldauf S.L., Leyval C., Straczek J. and Young J.P. 2002. Extensive fungal diversity in plant roots. Science 295, 2051.

Address for correspondence: Sergey A. Karpov. Zoological Institute RAS, Universitetskaya Emb. 1, 199034 St. Petersburg, Russia; e-mail: *sakarpov4@gmail.com*